

Facile Transformation of Isolated Fragments to Infinite Chains in Rhenium Chalcocyanide Clusters: Synthesis and Structure of $(\text{Pr}_4\text{N})_2M(\text{H}_2\text{O})_5[\text{Re}_6\text{X}_8(\text{CN})_6]\cdot\text{H}_2\text{O}$ and $(\text{Pr}_4\text{N})_2M(\text{H}_2\text{O})_4[\text{Re}_6\text{S}_8(\text{CN})_6]$ ($X = \text{S}, \text{Se}; M = \text{Mn}, \text{Ni}$)

N. G. Naumov,¹ S. B. Artemkina, A. V. Virovets, and V. E. Fedorov

Institute of Inorganic Chemistry, Russian Academy of Sciences, Novosibirsk 630090, Russia

Received December 27, 1999; in revised form March 31, 2000; accepted April 7, 2000; published online July 17, 2000

In this paper we report the synthesis of new compounds containing cluster anions $[\text{Re}_6\text{S}_8(\text{CN})_6]^{4-}$ and $[\text{Re}_6\text{Se}_8(\text{CN})_6]^{4-}$. Interaction of aqueous solutions of anions with transition metal cations in presence of Pr_4N^+ gives two type of compounds: $(\text{Pr}_4\text{N})_2M(\text{H}_2\text{O})_5[\text{Re}_6\text{X}_8(\text{CN})_6]\cdot\text{H}_2\text{O}$, $X = \text{S}, \text{Se}$ (orthorhombic phase) and $(\text{Pr}_4\text{N})_2M(\text{H}_2\text{O})_4[\text{Re}_6\text{S}_8(\text{CN})_6]$ (tetragonal phase), $X = \text{S}, \text{Se}$, $M = \text{Mn}, \text{Ni}$. The structures of $(\text{Pr}_4\text{N})_2\text{Mn}(\text{H}_2\text{O})_5[\text{Re}_6\text{Se}_8(\text{CN})_6]\cdot\text{H}_2\text{O}$ (space group: $P2_12_12_1$, $a = 18.286(2)$ Å, $b = 18.345(2)$ Å, $c = 16.568(2)$ Å, $V = 5558(1)$ Å³, $Z = 4$, $R1 = 0.0387$, $wR2 = 0.0624$), $(\text{Pr}_4\text{N})_2\text{Mn}(\text{H}_2\text{O})_4[\text{Re}_6\text{S}_8(\text{CN})_6]$ (space group: $I4/m$, $a = 13.255(2)$ Å, $c = 14.432(3)$ Å, $V = 2535.6(8)$ Å³, $R1 = 0.0369$, $wR2 = 0.0960$) and $(\text{Pr}_4\text{N})_2\text{Ni}(\text{H}_2\text{O})_4[\text{Re}_6\text{S}_8(\text{CN})_6]$ (space group: $I4/m$, $a = 13.247(4)$ Å, $c = 14.246(6)$ Å, $V = 2500(2)$ Å³, $R1 = 0.0414$, $wR2 = 0.1004$) were determined by X-ray single crystal analysis. The structure of $(\text{Pr}_4\text{N})_2\text{Mn}(\text{H}_2\text{O})_5[\text{Re}_6\text{Se}_8(\text{CN})_6]\cdot\text{H}_2\text{O}$ contains isolated fragments $\{\text{Mn}(\text{H}_2\text{O})_5[\text{Re}_6\text{Se}_8(\text{CN})_6]\}^{2-}$. The structures of $(\text{Pr}_4\text{N})_2M(\text{H}_2\text{O})_4[\text{Re}_6\text{S}_8(\text{CN})_6]$ ($M = \text{Mn}, \text{Ni}$) contain $\{\text{Mn}(\text{H}_2\text{O})_4[\text{Re}_6\text{S}_8(\text{CN})_6]\}^{2-}$ infinite chains. When heated the $(\text{Pr}_4\text{N})_2M(\text{H}_2\text{O})_5[\text{Re}_6\text{S}_8(\text{CN})_6]\cdot\text{H}_2\text{O}$ compounds transform into $(\text{Pr}_4\text{N})_2M(\text{H}_2\text{O})_4[\text{Re}_6\text{S}_8(\text{CN})_6]$, the reaction conditions depending on the nature of the metal. The formation and conversion of the compounds are discussed in terms of substitution of water molecules in coordination sphere of transition metal cations. It is shown that the orthorhombic structure can be considered as a superstructure in respect to the tetragonal one. © 2000 Academic Press

Key Words: rhenium; sulfur; selenium; cyanide; crystal structure.

1. INTRODUCTION

The ability of CN ligands to form stable complexes with transition metals is well known (1–3). In most cyano complexes the transition metal ions are coordinated with

the carbon atom of CN groups but in some complexes the metal ions can also coordinate via nitrogen. Besides, the cyanide anion CN^- is able to behave as a C,N-bridging ligand binding two coordination centers. Thus, the carbon-coordinated cyano complexes $[M(\text{CN})_n]$ can bind to another coordination center M' at the nitrogen atom forming separate $M\text{--CN--}M'$ fragments or $\text{--}M\text{--CN--}M'\text{--}$ chain structures. Prussian blue formed by the iron atoms bridged with CN ligands is the best known example of a polymeric structure.

The energy of $M\text{--CN}$ and $M\text{--NC}$ bonds is more negative as compared to that of $M\text{--OH}_2$ bonds; therefore, the interaction of cyano complexes $[M(\text{CN})_6]^{n-}$ with aqua complexes $[M'(\text{H}_2\text{O})_6]^{n+}$ leads to formation of compounds with $\text{--}M\text{--CN--}M'\text{--}$ bonds which often have polymeric nature. To prepare transition metal compounds with low dimensionality—layers, chains, or isolated fragments—the restriction of coordination abilities of transition metals is widely used (4–6).

From structural and chemical points of view the cluster anions $[\text{Re}_6\text{X}_8(\text{CN})_6]^{4-}$ ($X = \text{S}, \text{Se}, \text{Te}$) (7–10) can be considered as $[M(\text{CN})_6]^{n-}$ analogues. It was shown recently (11–15) that the interaction of these anions with aqua cations of 3d transition metals results in formation of polymeric 2D and 3D frameworks originating from $\text{Re--CN--}M\text{--NC--Re}$ interactions.

Here we report the synthesis of two new types of compounds: $(\text{Pr}_4\text{N})_2[M(\text{H}_2\text{O})_5][\text{Re}_6\text{X}_8(\text{CN})_6]\cdot\text{H}_2\text{O}$ ($M = \text{Mn}, \text{Ni}; X = \text{S}, \text{Se}$), having isolated ionic pairs, and $(\text{Pr}_4\text{N})_2[M(\text{H}_2\text{O})_4][\text{Re}_6\text{S}_8(\text{CN})_6]$ ($M = \text{Mn}, \text{Ni}$), having infinite one-dimensional chains. Phase transformation is discussed in terms of relationship of sub- and superstructures.

2. EXPERIMENTAL

2.1. Syntheses

Starting cluster compounds $\text{Cs}_3\text{K}[\text{Re}_6\text{S}_8(\text{CN})_6]\cdot 2\text{H}_2\text{O}$ and $\text{K}_4[\text{Re}_6\text{Se}_8(\text{CN})_6]\cdot 3.5\text{H}_2\text{O}$ were prepared from

¹To whom correspondence should be addressed. Fax: 3832-344489. E-mail: naumov@che.nsk.su.

polymeric $\text{Re}_6\text{S}_8\text{Br}_2$ (16) and $\text{Re}_6\text{Se}_8\text{Br}_2$ (17) as described in (8, 12). All other reagents were employed as purchased.

2.1.1. Preparation of $(\text{Pr}_4\text{N})_2\text{Mn}(\text{H}_2\text{O})_5[\text{Re}_6\text{S}_8(\text{CN})_6] \cdot \text{H}_2\text{O}$ (1). Aqueous solution of 0.200 g (0.10 mmol) of $\text{Cs}_3\text{KRe}_6\text{S}_8(\text{CN})_6 \cdot 2\text{H}_2\text{O}$ in 20 ml was gradually added to an aqueous mixture of 0.063 g of $n\text{-Pr}_4\text{NBr}$ (0.237 mmol) and 0.035 g of $\text{Mn}(\text{NO}_3)_2 \cdot 6\text{H}_2\text{O}$ (0.120 mmol) in 20 ml of water and stirred for 2 hours. Yellow-orange fine powder of **1** was filtered off, washed with water, and dried in air. Yield: 0.192 g (93%). X-ray: space group $P2_12_12_1$. Found (calcd) for $\text{C}_{30}\text{H}_{68}\text{N}_8\text{O}_6\text{S}_8\text{MnRe}_6$: C, 17.11% (17.44%); H, 3.16% (3.32%); N, 5.43% (5.47%); H_2O , 4.10% (5.23%). IR (KBr), cm^{-1} : 418 (w), $\text{M}-\text{C}\equiv\text{N}$; 1629 (m, br), H_2O ; 2127 (s), $\text{C}\equiv\text{N}$; 3434 (m, br), H_2O (bands of $n\text{-Pr}_4\text{N}^+$ are omitted). μ_{eff} (298 K) = 5.16 μ_{B} , μ_{eff} (4 K) = 4.95 μ_{B} .

2.1.2. Preparation of $(\text{Pr}_4\text{N})_2\text{Mn}(\text{H}_2\text{O})_4[\text{Re}_6\text{S}_8(\text{CN})_6] \cdot \text{H}_2\text{O}$ (2). 0.100 g portion of **1** and 0.5 ml of water were put into a quartz ampoule, which was then sealed and heated at 140°C for 2 days. Crystalline powder of **2** was collected and dried in air. Yield quantitative. Found (calcd) for $\text{C}_{30}\text{H}_{64}\text{N}_8\text{O}_4\text{S}_8\text{MnRe}_6$: C, 17.62% (17.75%); H, 3.26% (3.18%); N, 5.48% (5.52%); H_2O , 4.12% (3.54%). IR (KBr), cm^{-1} : 421 (w), $\text{M}-\text{C}\equiv\text{N}$; 1629 (m, br), H_2O ; 2118, 2154 (s), $\text{C}\equiv\text{N}$; 3635 (m, br), H_2O (bands of $n\text{-Pr}_4\text{N}^+$ are omitted). μ_{eff} (298 K) = 5.88 μ_{B} , μ_{eff} (4 K) = 5.80 μ_{B} .

2.1.3. Preparation of $(\text{Pr}_4\text{N})_2\text{Mn}(\text{H}_2\text{O})_5[\text{Re}_6\text{Se}_8(\text{CN})_6] \cdot \text{H}_2\text{O}$ (3). The material was prepared as a fine orange powder in a manner similar to the preparation of **1** except for the use of $\text{K}_4\text{Re}_6\text{Se}_8(\text{CN})_6 \cdot 3.5\text{H}_2\text{O}$ (0.212 g, 0.1000 mmol) instead of $\text{Cs}_3\text{KRe}_6\text{S}_8(\text{CN})_6 \cdot 2\text{H}_2\text{O}$. Yield: 0.232 g (95%), X-ray: space group $P2_12_12_1$. Found (calcd) for $\text{C}_{30}\text{H}_{68}\text{N}_8\text{O}_6\text{Se}_8\text{MnRe}_6$: C, 14.93% (14.76%); H, 3.00% (2.81%); N, 4.41% (4.59%); H_2O , 4.87% (4.42%). IR (KBr), cm^{-1} : 415 (w), $\text{M}-\text{C}\equiv\text{N}$; 1620, 1629 (m), H_2O ; 2113.0 (s), 2123 (sh), 2141 (sh), $\text{C}\equiv\text{N}$; 3637 cm^{-1} (m, br), H_2O (bands of $n\text{-Pr}_4\text{N}^+$ are omitted). μ_{eff} (298 K) = 5.436 μ_{B} , μ_{eff} (4 K) = 5.30 μ_{B} .

2.1.4. Preparation of $(\text{Pr}_4\text{N})_2\text{Ni}(\text{H}_2\text{O})_5[\text{Re}_6\text{S}_8(\text{CN})_6] \cdot \text{H}_2\text{O}$ (4). The material was prepared as a fine orange powder in a manner similar to the preparation of **1** except for the use of $\text{Ni}(\text{CH}_3\text{COO})_2 \cdot 4\text{H}_2\text{O}$ (0.030 g, 0.12 mmol) instead of $\text{Mn}(\text{NO}_3)_2 \cdot 6\text{H}_2\text{O}$. Yield: 0.232 g (97%). X-ray: space group $P2_12_12_1$. Found (calcd) for $\text{C}_{30}\text{H}_{68}\text{N}_8\text{O}_6\text{S}_8\text{NiRe}_6$: C, 14.98% (14.76%); H, 3.11% (2.81%); N, 4.40% (4.59%); H_2O , 5.00% (5.21%). IR (KBr), cm^{-1} : 417 (w), $\text{M}-\text{C}\equiv\text{N}$; 1621 (m), H_2O ; 2122.0 (s), 2133 (s), 2150 (m), 2168 (m, sh), $\text{C}\equiv\text{N}$; 3575, 3596, 3624 (m,br), H_2O (bands of $n\text{-Pr}_4\text{N}^+$ are omitted). μ_{eff} (298 K) = 3.16 μ_{B} , μ_{eff} (77 K) = 3.10 μ_{B} .

2.1.5. Preparation of $(\text{Pr}_4\text{N})_2\text{Ni}(\text{H}_2\text{O})_4[\text{Re}_6\text{S}_8(\text{CN})_6] \cdot \text{H}_2\text{O}$ (5). A 0.100 g portion of **4** was boiled in water for 1 day. Fine powder of **5** was filtered off and dried in air. Yield:

quantitative. X-ray: space group $I4/m$. Found (calcd) for $\text{C}_{30}\text{H}_{64}\text{N}_8\text{O}_4\text{NiRe}_6$: C, 17.85% (17.75%); H, 3.25% (3.18%); N, 5.60% (5.52%); H_2O , 3.19% (3.54%). IR (KBr), cm^{-1} : 421 (w), $\text{M}-\text{C}\equiv\text{N}$; 1617 (m, br), H_2O ; 2114 (s), 2166 (s), $\text{C}\equiv\text{N}$; 3643 (m, br), H_2O (bands of $n\text{-Pr}_4\text{N}^+$ are omitted). μ_{eff} (298 K) = 3.12 μ_{B} , μ_{eff} (77 K) = 3.10 μ_{B} .

2.1.6. Preparation of $(\text{Pr}_4\text{N})_2\text{Ni}(\text{H}_2\text{O})_5[\text{Re}_6\text{Se}_8(\text{CN})_6] \cdot \text{H}_2\text{O}$ (6). The material was prepared as a fine orange powder in a manner similar to the preparation of **1** from $\text{K}_4\text{Re}_6\text{Se}_8(\text{CN})_6 \cdot 3.5\text{H}_2\text{O}$ (0.212 g, 0.100 mmol) and of $\text{Ni}(\text{CH}_3\text{COO})_2 \cdot 4\text{H}_2\text{O}$ (0.030 g, 0.12 mmol). Yield: 0.232 g (95%). X-ray: space group $P2_12_12_1$. Found (calcd) for $\text{C}_{30}\text{H}_{68}\text{N}_8\text{O}_6\text{Se}_8\text{NiRe}_6$: C, 14.89% (14.76%); H, 3.15% (2.81%); N, 4.55% (4.59%); H_2O , 4.64% (4.42%). IR (KBr), cm^{-1} : 410 (w), $\text{M}-\text{C}\equiv\text{N}$; 1616 (w), H_2O ; 2114.0 (s, br), 2130, $\text{C}\equiv\text{N}$; 2969.0 (m), 3637.0 (m, br), H_2O (bands of $n\text{-Pr}_4\text{N}^+$ are omitted). μ_{eff} (298 K) = 3.10 μ_{B} , μ_{eff} (77 K) = 3.25 μ_{B} .

2.1.7. Single-crystal growth. All compounds have extremely low solubility, and therefore crystals suitable for X-ray single-crystal analysis were grown by diffusion of reagents coming from opposite directions in a U-tube filled with silica gel. To prepare the silica gel a solution of 12.25 g of $\text{Na}_2\text{SiO}_3 \cdot 9\text{H}_2\text{O}$ in 50 ml of water was titrated with 20 ml of 1 M HCl under vigorous stirring. The resulting mixture was placed into U-tubes and the gel allowed to set for 2 days.

The aqueous mixture of Pr_4NBr (0.1 M) and $[\text{M}(\text{H}_2\text{O})_6]^{2+}$ (0.1 M) and an aqueous solution of $[\text{Re}_6\text{X}_8(\text{CN})_6]^{4-}$ (0.1 M) were put into two sections of the U-tube. Diffusion of reagents through silica gel for 4–6 weeks resulted in crystals suitable for X-ray single-crystal determination. Crystals were located near the middle part of the tube. The following reagents were used: **2**, $\text{Mn}(\text{NO}_3)_2 \cdot 6\text{H}_2\text{O}$, $\text{Cs}_3\text{K}[\text{Re}_6\text{S}_8(\text{CN})_6] \cdot 2\text{H}_2\text{O}$; **3**, $\text{Mn}(\text{NO}_3)_2 \cdot 6\text{H}_2\text{O}$, $\text{K}_4[\text{Re}_6\text{Se}_8(\text{CN})_6] \cdot 3.5\text{H}_2\text{O}$; **5**, $\text{Ni}(\text{CH}_3\text{COO})_2 \cdot 4\text{H}_2\text{O}$, $\text{Cs}_3\text{K}[\text{Re}_6\text{S}_8(\text{CN})_6] \cdot 2\text{H}_2\text{O}$. Octahedral or prismatic crystals can be easily separated from silica gel manually. X-ray powder diffraction and IR spectroscopy revealed these crystals to be identical with powder samples.

2.1.8. Physical measurements. Elemental analyses for C, H, N, and S (Carlo Erba 1106) were performed in the Laboratory of Microanalysis at the Institute of Organic Chemistry, Novosibirsk. Infrared spectra were measured on KBr disks with a Bruker IFS-85 spectrometer. To determine the water content the curves of weight loss were recorded at a heating rate of 3°C/min (temperature range 20–300°C) in argon atmosphere with a TGD-7000 RH thermal analysis controller (Sinku-Riku, Japan). Magnetic measurements were performed using a SQUID magnetometer from Quantum Design in a range 2–300 K, field 5 kOe. The X-ray powder diffraction data (XPD) were obtained with a Philips

TABLE 1
Crystallographic Data for Compounds $(\text{Pr}_4\text{N})_2\text{Mn}(\text{H}_2\text{O})_4[\text{Re}_6\text{S}_8(\text{CN})_6]$ (2), $(\text{Pr}_4\text{N})_2\text{Mn}(\text{H}_2\text{O})_5[\text{Re}_6\text{S}_8(\text{CN})_6] \cdot \text{H}_2\text{O}$ (3), and $(\text{Pr}_4\text{N})_2\text{Ni}(\text{H}_2\text{O})_4[\text{Re}_6\text{S}_8(\text{CN})_6]$ (5)

	2	3	5
Empirical formula	$\text{C}_{30}\text{H}_{64}\text{MnN}_8\text{O}_4\text{Re}_6\text{S}_8$	$\text{C}_{30}\text{H}_{68}\text{MnN}_8\text{O}_6\text{Re}_6\text{S}_8$	$\text{C}_{30}\text{H}_{64}\text{N}_8\text{NiO}_4\text{Re}_6\text{S}_8$
Formula weight	2029.51	2440.74	2033.28
Color, habit	Red, octahedral	Red, prismatic	Red, octahedral
Crystal system	Tetragonal	Orthorhombic	Tetragonal
Space group	$I4/m$	$P2_12_12_1$	$I4/m$
a , Å	13.255(2)	18.286(2)	13.247(4)
b , Å		18.345(2)	
c , Å	14.432(3)	16.568(2)	14.246(6)
Cell volume, Å ³	2535.6(8)	5558(1)	2500(2)
Z	2	4	2
Exp. hkl limits	$0 < h < 15$ $0 < k < 15$ $0 < l < 17$	$0 < h < 21$ $0 < k < 21$ $0 < l < 19$	$0 < h < 17$ $0 < k < 17$ $0 < l < 18$
Calc. density, g·cm ⁻³	2.658	2.917	2.701
Absorption correction	3 azimuthal scan curves	4 azimuthal scan curves	3 azimuthal scan curves
Absorption coefficient, mm ⁻¹	14.872	18.514	15.208
Crystal size, mm	$0.40 \times 0.36 \times 0.24$	$0.34 \times 0.32 \times 0.28$	$0.24 \times 0.21 \times 0.20$
$2\theta_{\text{max}}$, deg	50	50	56
Reflections collected/unique	1191/1094 [$R_{\text{int}} = 0.0424$]	3572/3572	1480/1372 [$R_{\text{int}} = 0.0525$]
Goodness-of-fit on F^2	1.004	0.511	0.885
Final R indices	$R1 = 0.0369$,	$R1 = 0.0387$,	$R1 = 0.0414$,
$[I > 2\sigma(I)]$	$wR2 = 0.0960$	$wR2 = 0.0624$	$wR2 = 0.1004$
Weighting scheme	$w^{-1} = \sigma^2(F_o^2) + (0.0632P)^2$	$w^{-1} = \sigma^2(F_o^2) + (0.0134P)^2$	$w^{-1} = \sigma^2(F_o^2) + (0.0504P)^2$
Max., min. peak in final diff. map, e ⁻ ·Å ⁻³	2.449, - 2.810	1.91, - 1.99	1.95, - 3.49

APD 1700 powder diffractometer with silicon as internal standard (step, 0.03°; sample time, 0.5 sec; 2θ range, 5–60°; radiation, $\text{CuK}\alpha$).

2.1.9. Structural studies of compounds 2, 3, and 5. The intensity data were collected on an Enraf-Nonius CAD4 diffractometer with graphite-monochromated $\text{MoK}\alpha$ radiation ($\lambda = 0.71073$ Å) under ambient conditions ($T = 291$ K). The cell parameters were refined using setting angles of 24 precisely positioned reflections with $9 < \theta < 15^\circ$. Reflection intensities were collected by standard techniques ($\theta/2\theta$ scans with variable speed, ω range (deg) = $0.9 + 0.35 \text{tg}(\theta)$). Absorption corrections were applied by measuring the azimuthal scan curves. The structures were solved by direct methods and refined by full-matrix least-squares fit on F^2 for all data. Anisotropic displacement parameters (adp) were refined for all nonhydrogen atoms. The final difference electron density map contained no chemically reasonable peaks. The crystal data are listed in Table 1. The calculations were performed with standard Enraf-Nonius CAD4 programs (CD4CA0, CADSDAT), SIR97 (18) (structure solution for 3), and SHELX-97 (19) (structure solution for 2 and 5 and refinement for all). Atomic coordinates and equivalent isotropic displacement

parameters are listed in Tables 2–4, and selected bond lengths and angles in Table 5.

3. RESULTS AND DISCUSSION

3.1. Synthesis

The interaction of aqueous solutions of $n\text{-Pr}_4\text{N}^+$, $M(\text{H}_2\text{O})_6^{2+}$ ($M = \text{Mn}, \text{Ni}$), and $[\text{Re}_6\text{S}_8(\text{CN})_6]^{4-}$ gives two types of compounds with analogous compositions: $(\text{Pr}_4\text{N})_2M(\text{H}_2\text{O})_5[\text{Re}_6\text{S}_8(\text{CN})_6] \cdot \text{H}_2\text{O}$ (1 and 4) and $(\text{Pr}_4\text{N})_2M(\text{H}_2\text{O})_4[\text{Re}_6\text{S}_8(\text{CN})_6]$ (2 and 5). At ambient temperature the reaction results in fast precipitation of the $(\text{Pr}_4\text{N})_2M(\text{H}_2\text{O})_5[\text{Re}_6\text{S}_8(\text{CN})_6] \cdot \text{H}_2\text{O}$ regardless of concentrations and ratio of reagents. Stirring over 1 week does not give any $(\text{Pr}_4\text{N})_2M(\text{H}_2\text{O})_4[\text{Re}_6\text{S}_8(\text{CN})_6]$. According to the data of powder diffraction investigation compounds 1 and 4 are isostructural to previously investigated $(\text{Pr}_4\text{N})_2\text{Co}(\text{H}_2\text{O})_5[\text{Re}_6\text{S}_8(\text{CN})_6] \cdot \text{H}_2\text{O}$ (20) (Fig. 1) with close cell parameters.

The transformation of $(\text{Pr}_4\text{N})_2M(\text{H}_2\text{O})_5[\text{Re}_6\text{S}_8(\text{CN})_6] \cdot \text{H}_2\text{O}$ into $(\text{Pr}_4\text{N})_2M(\text{H}_2\text{O})_4[\text{Re}_6\text{S}_8(\text{CN})_6]$ occurs at elevated temperatures but the rate of the process depends on the nature of the metal. The transformation completes in 2 hours in the case of nickel and requires boiling during

TABLE 2
Atomic Coordinates ($\times 10^4$) and Equivalent Isotropic Displacement Parameters ($\text{\AA}^2 \times 10^3$) for **2**

	x	y	z	U_{eq}
Re(1)	0	0	1270(1)	22(1)
Re(2)	520(1)	1288(1)	0	23(1)
S(1)	1662(2)	706(2)	1172(2)	33(1)
Mn(1)	0	0	5000	37(1)
O(1)	1511(10)	725(11)	5000	71(4)
C(1)	0	0	2704(13)	32(5)
N(1)	0	0	3492(14)	45(5)
C(2)	1144(12)	2757(12)	0	34(4)
N(2)	1519(13)	3546(12)	0	58(5)
N(11)	5000	0	2500	38(5)
C(11)	4548(9)	804(9)	1864(8)	43(3)
C(12)	4017(9)	1646(9)	2352(10)	48(3)
C(13)	3756(10)	2466(9)	1649(11)	61(4)

Note. U_{eq} is defined as one-third of the trace of the orthogonalized U_{ij} tensor.

1 day for cobalt. In the case of manganese this reaction occurs only at 140°C in a sealed ampoule. Figure 2 demonstrates this transformation for the manganese compound.

In the case of a selenium cluster only $(\text{Pr}_4\text{N})_2\text{M}(\text{H}_2\text{O})_5[\text{Re}_6\text{Se}_8(\text{CN})_6] \cdot \text{H}_2\text{O}$ ($M = \text{Mn}$ (**3**), Ni (**6**)) compounds were isolated and no traces of $(\text{Pr}_4\text{N})_2\text{M}(\text{H}_2\text{O})_4[\text{Re}_6\text{Se}_8(\text{CN})_6]$ were detected.

3.2. Structure Description

The structures of cluster anions $[\text{Re}_6\text{S}_8(\text{CN})_6]^{4-}$ and $[\text{Re}_6\text{Se}_8(\text{CN})_6]^{4-}$ are presented in Figs. 3a,b. These anions have the usual $\text{Re}_6X_8L_6$ environment. Six rhenium atoms form an Re_6 octahedron with the faces μ_3 -capped by eight chalcogen atoms. The CN ligands are coordinated to rhenium atoms via carbon. Bond distances and angles in these anions (Table 5) do not differ from those found in other salts with the Re_6X_8 cluster core ($\text{Cs}_2\text{Co}[\text{Re}_6\text{S}_8(\text{CN})_6] \cdot 2\text{H}_2\text{O}$ (**12**): Re–Re, 2.599; Re–S, 2.411; Re–C, 2.12; C–N, 1.14; $\text{NaCs}_3\text{Re}_6\text{S}_8(\text{CN})_6$ (**14**): Re–Re, 2.602; Re–S, 2.413; Re–C, 2.12; C–N, 2.16; $\text{Cs}_5\text{Re}_6\text{S}_8\text{Cl}_7$ (**21**): Re–Re, 2.597; Re–S, 2.399; $\text{K}_4[\text{Re}_6\text{Se}_8(\text{CN})_6] \cdot 3.5\text{H}_2\text{O}$ (**8**): Re–Re, 2.633; Re–Se, 2.526; Re–C, 2.11; C–N, 1.15; $\text{NaCs}_3\text{Re}_6\text{Se}_8(\text{CN})_6$ (**14**): Re–Re, 2.634; Re–Se, 2.52; Re–C, 2.10; C–N, 2.17; $\text{Cs}_4\text{Re}_6\text{Se}_8\text{I}_6$ (**21**): Re–Re, 2.625; Re–Se, 2.519 (in \AA)).

3.2.1. Structures of $(n\text{-Pr}_4\text{N})_2\text{M}(\text{H}_2\text{O})_4[\text{Re}_6\text{S}_8(\text{CN})_6]$ ($M = \text{Mn}, \text{Ni}$). The compounds $(n\text{-Pr}_4\text{N})_2\text{Mn}(\text{H}_2\text{O})_4[\text{Re}_6\text{S}_8(\text{CN})_6]$ (**2**) and $(n\text{-Pr}_4\text{N})_2\text{Ni}(\text{H}_2\text{O})_4[\text{Re}_6\text{S}_8(\text{CN})_6]$ (**5**) are isostructural and crystallize in the $I4/m$ space group. The structure of $(n\text{-Pr}_4\text{N})_2\text{Mn}(\text{H}_2\text{O})_4[\text{Re}_6\text{S}_8(\text{CN})_6]$ is given in Fig. 4. In this compound the coordination environment of

TABLE 3
Atomic Coordinates ($\times 10^4$) and Equivalent Isotropic Displacement Parameters ($\text{\AA}^2 \times 10^3$) for **3**

	x	y	z	U_{eq}
Re(1)	4950(2)	8955(2)	4974(2)	18(1)
Re(2)	4941(2)	10005(2)	6056(1)	19(1)
Re(3)	4020(2)	10034(2)	4854(2)	19(1)
Re(4)	5106(2)	9934(2)	3822(1)	17(1)
Re(5)	6039(2)	9905(2)	5030(2)	16(1)
Re(6)	5097(2)	10980(2)	4907(2)	21(1)
Se(1)	5853(5)	8993(6)	6126(6)	30(2)
Se(2)	5959(5)	10910(5)	6071(6)	25(2)
Se(3)	4198(5)	10968(5)	3751(6)	27(2)
Se(4)	3927(6)	9080(6)	5961(6)	30(2)
Se(5)	4073(5)	9047(5)	3808(6)	27(2)
Se(6)	4038(5)	11025(6)	5883(6)	33(2)
Se(7)	6138(5)	10832(5)	3926(5)	23(2)
Se(8)	5989(5)	8907(5)	3995(5)	21(2)
Mn(1)	4870(4)	9981(6)	600(4)	27(2)
C(1)	4720(50)	7800(50)	5160(50)	80(30)
N(1)	4870(30)	7180(20)	4900(40)	51(15)
C(2)	4880(40)	10040(50)	7360(30)	40(15)
N(2)	4840(30)	10030(40)	8070(20)	38(13)
C(3)	2840(20)	10090(30)	4820(20)	7(10)
N(3)	2250(30)	10110(30)	4820(30)	38(14)
C(4)	5130(30)	9930(30)	2430(20)	7(9)
N(4)	5160(30)	9870(30)	1810(20)	28(12)
C(5)	7200(30)	9750(30)	5070(40)	40(16)
N(5)	7790(30)	9790(30)	5040(30)	32(13)
C(6)	5180(40)	12200(30)	4850(30)	23(14)
N(6)	5390(20)	12740(20)	4830(30)	27(11)
O(1)	5468(17)	9036(18)	50(30)	43(10)
O(2)	5733(19)	10626(18)	50(30)	47(10)
O(3)	4240(20)	10320(20)	– 450(20)	45(11)
O(4)	4470(20)	11050(20)	1000(30)	61(14)
O(5)	4020(30)	9190(30)	750(40)	100(20)
O(1W)	6170(40)	9430(30)	– 1080(40)	140(30)
N(11)	2970(20)	2030(30)	8460(30)	20(13)
C(111)	2760(70)	1180(40)	8430(70)	160(50)
C(112)	2600(50)	840(40)	7490(40)	70(30)
C(113)	2480(40)	100(60)	7330(40)	60(20)
C(121)	3620(30)	2350(30)	7940(30)	25(15)
C(122)	4311(19)	2010(20)	8070(20)	0(9)
C(123)	4940(40)	2590(40)	7240(30)	60(20)
C(131)	2370(50)	2620(50)	8340(50)	100(30)
C(132)	1910(50)	3190(50)	9090(60)	110(30)
C(133)	1470(30)	3480(30)	8300(30)	22(14)
C(141)	3110(40)	2100(40)	9370(30)	50(20)
C(142)	2640(40)	2120(30)	9920(40)	60(20)
C(143)	2860(60)	2250(60)	10700(60)	100(40)
N(21)	7880(20)	1970(20)	6600(30)	25(14)
C(211)	8560(50)	2260(70)	7100(70)	150(50)
C(212)	8850(100)	1750(100)	6510(120)	520(130)
C(213)	9770(30)	2340(30)	7500(50)	48(18)
C(221)	7820(30)	1170(30)	6860(40)	33(16)
C(222)	7530(30)	1080(30)	7430(30)	25(15)
C(223)	7490(30)	200(30)	7530(30)	19(14)
C(231)	7220(20)	2390(30)	6870(30)	11(12)
C(232)	7200(40)	3200(40)	6680(50)	70(30)
C(233)	6400(60)	3830(60)	6450(60)	70(50)
C(241)	8120(70)	2210(70)	5710(50)	150(60)
C(242)	7480(30)	1820(30)	5010(40)	45(16)
C(243)	7750(40)	2130(50)	4240(50)	60(20)

Note. U_{eq} is defined as one-third of the trace of the orthogonalized U_{ij} tensor.

TABLE 4
Atomic Coordinates ($\times 10^4$) and Equivalent Isotropic Displacement Parameters ($\text{\AA}^2 \times 10^3$) for 5

	<i>x</i>	<i>y</i>	<i>z</i>	<i>U</i> _{eq}
Re(1)	0	0	1286(1)	21(1)
Re(2)	531(1)	1283(1)	0	21(1)
S(1)	1665(2)	689(3)	1193(2)	28(1)
Ni(1)	0	0	5000	53(2)
O(1)	1464(1)	689(13)	5000	65(5)
C(1)	0	0	2730(20)	33(7)
N(1)	0	0	3571(16)	37(6)
C(2)	1172(2)	2752(15)	0	36(5)
N(2)	1554(18)	3515(16)	0	76(8)
N(11)	5000	0	2500	28(5)
C(11)	4544(11)	794(10)	1851(10)	36(3)
C(12)	4023(12)	1658(11)	2329(11)	46(4)
C(13)	3763(12)	2459(11)	1625(12)	53(5)

Note. *U*_{eq} is defined as one-third of the trace of the orthogonalized *U*_{ij} tensor.

Mn²⁺ is built from four water molecules and two cyanide nitrogen atoms in *trans* positions. This type of binding leads to formation of extended negatively charged chains $-\text{NC}-[\text{Re}_6\text{S}_8(\text{CN})_4]\text{CN}-\text{M}(\text{H}_2\text{O})_4-\text{NC}-[\text{Re}_6\text{S}_8(\text{CN})_4]-\text{C N}-$ along the *c* axis (Fig. 4a). These chains are located on the four-fold axes. Polymeric chains are arranged with a shift along the body diagonal of the unit cell. Rather short $\text{CN}\cdots\text{O}(\text{H}_2\text{O})$ (2.83 Å) contacts are formed in the *xy* plane. The negative charge of the $\{-\text{Mn}(\text{H}_2\text{O})_4-[\text{Re}_6\text{S}_8(\text{CN})_6]_3\}^{2-}$ chains is compensated by Pr_4N^+ cations located between the chains (Fig. 4b). The *M*-O and *M*-N distances in compounds $(n-\text{Pr}_4\text{N})_2\text{Mn}(\text{H}_2\text{O})_4[\text{Re}_6\text{S}_8(\text{CN})_6]$ and $(n-\text{Pr}_4\text{N})_2\text{Ni}(\text{H}_2\text{O})_4[\text{Re}_6\text{S}_8(\text{CN})_6]$

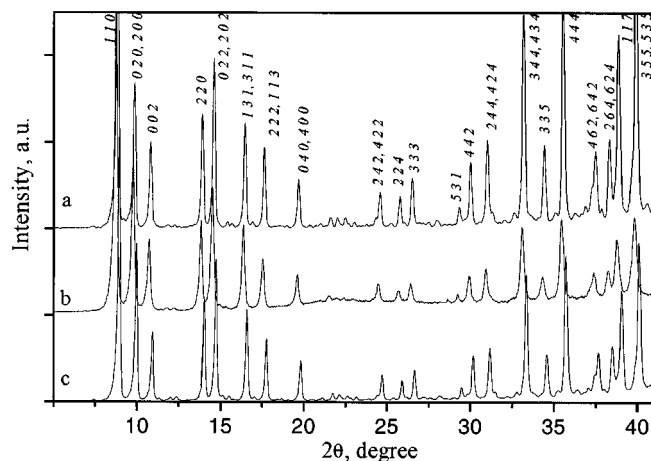


FIG. 1. Indexed X-ray powder diffraction patterns for $(\text{Pr}_4\text{N})_2\text{M}(\text{H}_2\text{O})_5[\text{Re}_6\text{S}_8\text{CN}_6] \cdot \text{H}_2\text{O}$: (a) *M* = Co (Ref. 20), (b) *M* = Mn (1), (c) *M* = Ni (4).

(Table 5) are typical for these metal ions in an octahedral environment.

3.2.2. Structure of $(n-\text{Pr}_4\text{N})_2\text{Mn}(\text{H}_2\text{O})_5[\text{Re}_6\text{S}_8(\text{CN})_6] \cdot \text{H}_2\text{O}$. The compound $(n-\text{Pr}_4\text{N})_2\text{Mn}(\text{H}_2\text{O})_5[\text{Re}_6\text{S}_8(\text{CN})_6] \cdot \text{H}_2\text{O}$ crystallizes in space group $P2_12_12_1$ and contains isolated fragments $\{\text{Mn}(\text{H}_2\text{O})_5[\text{Re}_6\text{S}_8(\text{CN})_6]\}^{2-}$. The coordination environment of Mn atom consists of five water molecules and one cyano ligand belonging to the $[\text{Re}_6\text{S}_8(\text{CN})_6]^{4-}$ anion, the cyanide being N-bound (Fig. 5a). These fragments are arranged along the *c* direction forming hydrogen bonds between the *trans* water molecule O3 of the Mn coordination sphere and nitrogen atom N2' of the next $\{\text{Mn}(\text{H}_2\text{O})_5[\text{Re}_6\text{S}_8(\text{CN})_6]\}^{2-}$ fragment. The

TABLE 5
Selected Bond Lengths and Angles for Compounds $(\text{Pr}_4\text{N})_2\text{Mn}(\text{H}_2\text{O})_4[\text{Re}_6\text{S}_8(\text{CN})_6]$ (2), $(\text{Pr}_4\text{N})_2\text{Mn}(\text{H}_2\text{O})_5[\text{Re}_6\text{S}_8(\text{CN})_6] \cdot \text{H}_2\text{O}$ (3), and $(\text{Pr}_4\text{N})_2\text{Ni}(\text{H}_2\text{O})_4[\text{Re}_6\text{S}_8(\text{CN})_6]$ (5) (Min. -Max.; Mean)

	2	3	5
Bond Lengths, Å			
Re-Re	2.5972(7)-2.6034(9); 2.6003	2.609(5)-2.647(5); 2.629	2.596(1)-2.602(1); 2.599
Re-X	2.397(3)-2.398(3); 2.398	2.49(1)-2.54(1); 2.51	2.391(3)-2.401(3); 2.397
Re-C	2.07(2)-2.12(2); 2.10	2.14(6)-2.31(3); 2.20	2.06(3)-2.12(2); 2.09
M-N	2.18(2)	2.08(4)	2.04(2)
M-O	2.22(1)	2.14(6)-2.24(4); 2.19	2.14(2)
C-N	1.14(3)-1.16(2); 1.15	1.03(4)-1.24(8); 1.11	1.13(3)-1.20(3); 1.17
Bond Angles, °			
∠(N-M-O)	90.0	83(2)-106(2); 95	90.0
∠(N-M-O) (<i>trans</i>)	180.0	159(2)	180.0
∠(O-M-O)	90.0	79(2)-109(2); 88	90.0
∠(O-M-O) (<i>trans</i>)	180.0(7)	161(2)-168(2); 165	180.0
∠(Re-C-N)	178(2)-180.0; 179	142(7)-168(6); 167	177(2)-180.0; 179
∠(M-N-C)	180.0	158(5)	180.0

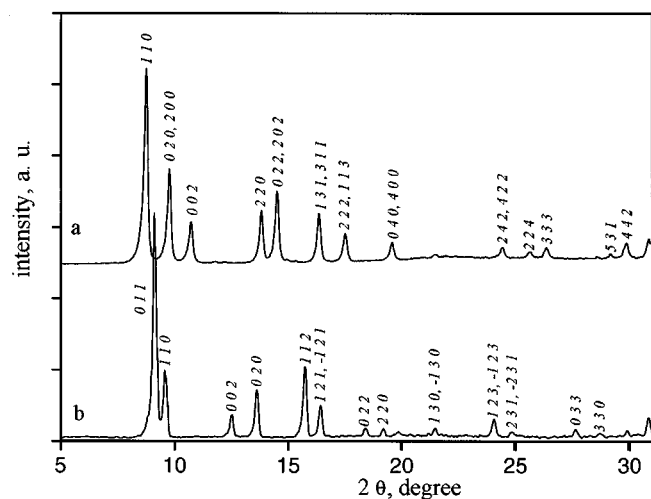


FIG. 2. Indexed X-ray powder diffraction patterns of (a) $(\text{Pr}_4\text{N})_2\text{Mn}(\text{H}_2\text{O})_5[\text{Re}_6\text{S}_8(\text{CN})_6]\cdot\text{H}_2\text{O}$ and (1) (b) $(\text{Pr}_4\text{N})_2\text{Mn}(\text{H}_2\text{O})_4[\text{Re}_6\text{S}_8(\text{CN})_6]$ (2).

equatorial O1, O2, O4, and O5 water molecules also form hydrogen bonds the neighboring fragments ($\text{O}\cdots\text{N}$ distance 2.7–3.0 Å). The tetrapropylammonium cations are located between these fragments compensating their negative charge (Fig. 5b).

The $M\text{--O}$ and $M\text{--N}$ distances in $(n\text{-Pr}_4\text{N})_2\text{Mn}(\text{H}_2\text{O})_5[\text{Re}_6\text{S}_8(\text{CN})_6]\cdot\text{H}_2\text{O}$ (3) (Table 5) correspond

to those found in $(n\text{-Pr}_4\text{N})_2\text{Mn}(\text{H}_2\text{O})_4[\text{Re}_6\text{S}_8(\text{CN})_6]$ (2) and the typical for the manganese(II) ion in an octahedral environment. This compound is isostructural with $(n\text{-Pr}_4\text{N})_2\text{Co}(\text{H}_2\text{O})_5[\text{Re}_6\text{S}_8(\text{CN})_6]\cdot\text{H}_2\text{O}$ recently reported by us (20). In the unit cell the $[\text{Re}_6\text{S}_8]$ cluster cores form a *pseudo-face-centered* packing motif within the frame of a *pseudo- $F4/mmm$* space group, whereas light atoms (C, N, O, and H) belong to the noncentrosymmetrical chiral $P2_12_12_1$ space group. The presence of such pseudosymmetry is an interesting feature of this structure. In the diffraction patterns one observes two groups of reflections: $A = \{uuu, ggg\}$ (u means odd hkl index, g even) and $B = \{guu, ugu, uug, ggu, gug, ugg\}$. The A group contains reflections allowed by the F cell symmetry. These reflections have intensities 100–1000 times higher than those found for the B group (superstructural reflections). Obviously, this is the result of *pseudo- F* packing of the heavy atoms. This phenomenon causes difficulties in solution of the structure and the refinement of light atom positions, especially in Pr_4N^+ . It results in some unusual C–N distances like 1.24(8) Å (Table 5).

3.2.3. *Relationship of the structures.* The compounds $(n\text{-Pr}_4\text{N})_2M(\text{H}_2\text{O})_4[\text{Re}_6X_8(\text{CN})_6]$ and $(n\text{-Pr}_4\text{N})_2M(\text{H}_2\text{O})_5[\text{Re}_6X_8(\text{CN})_6]\cdot\text{H}_2\text{O}$ have similar structures. Despite having different space groups ($I4/m$ and $P2_12_12_1$), the packing motifs of the cluster anions are alike. The orthorhombic $(\text{Pr}_4\text{N})_2M(\text{H}_2\text{O})_5[\text{Re}_6X_8(\text{CN})_6]\cdot\text{H}_2\text{O}$ structure can be considered as a superstructure with respect to the

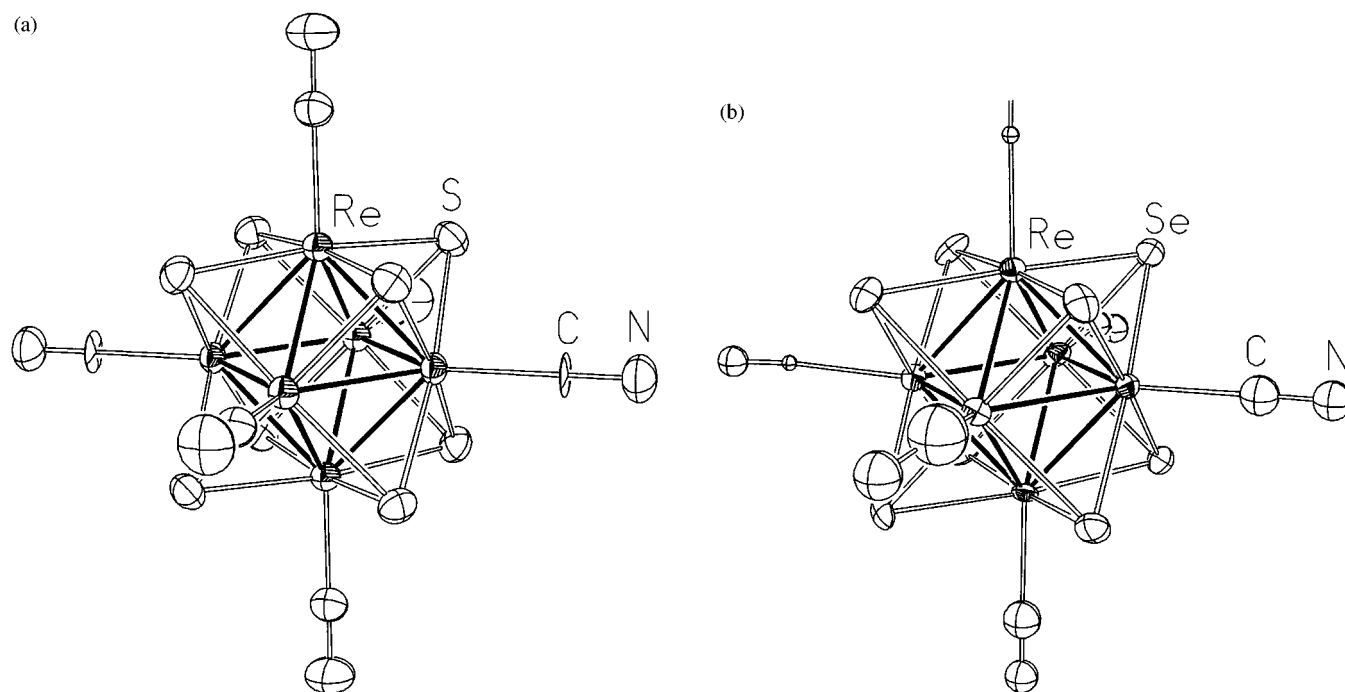


FIG. 3. Cluster anions $[\text{Re}_6\text{S}_8(\text{CN})_6]^{4-}$ and $[\text{Re}_6\text{Se}_8(\text{CN})_6]^{4-}$ in the compounds 2 (a) and 3 (b); 50% probability ellipsoids.

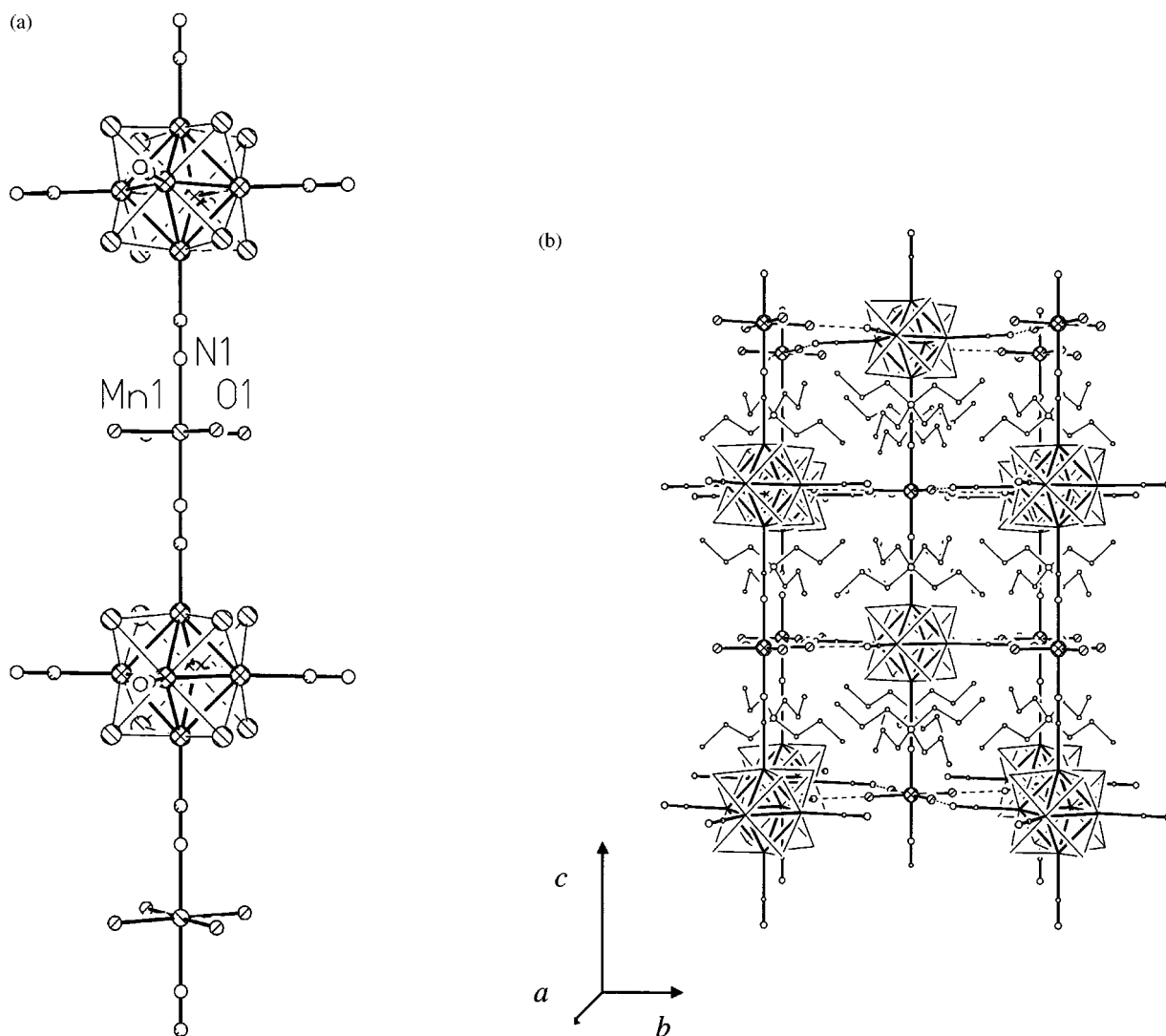


FIG. 4. Structure of $(\text{Pr}_4\text{N})_2\text{Mn}(\text{H}_2\text{O})_4[\text{Re}_6\text{S}_8(\text{CN})_6]$. (a) Infinite chains of $\{\text{Mn}(\text{H}_2\text{O})_4[\text{Re}_6\text{S}_8(\text{CN})_6]\}_\infty^{2-}$ running along the c direction. (b) Packing of chains and Pr_4N^+ cations in yz projection. Hydrogen bonds are shown as dashed lines.

tetragonal $(\text{Pr}_4\text{N})_2M(\text{H}_2\text{O})_4[\text{Re}_6\text{S}_8(\text{CN})_6]$. The unit cell transformation is depicted in Fig. 6. In the structure of $(n\text{-Pr}_4\text{N})_2M(\text{H}_2\text{O})_5[\text{Re}_6\text{X}_8(\text{CN})_6] \cdot \text{H}_2\text{O}$ the cluster cores follow a tetragonal F -centered motif (see above) with the geometry very close to an I -centered unit cell of smaller volume, the cell transformation vector being $\mathbf{a}' = \mathbf{a}/2 + \mathbf{b}/2$, $\mathbf{b}' = \mathbf{a}/2 - \mathbf{b}/2$, $\mathbf{c}' = \mathbf{c}$ (Fig. 6).

Taking into account experimental evidence that $(\text{Pr}_4\text{N})_2M(\text{H}_2\text{O})_5[\text{Re}_6\text{S}_8(\text{CN})_6] \cdot \text{H}_2\text{O}$ compounds ($M = \text{Mn}$, **1**; $M = \text{Ni}$, **4**) are isostructural with the Co analogue reported previously (20), the following model of $(\text{Pr}_4\text{N})_2\text{Mn}(\text{H}_2\text{O})_5[\text{Re}_6\text{S}_8(\text{CN})_6] \cdot \text{H}_2\text{O}$ (**1**) \rightarrow $(\text{Pr}_4\text{N})_2\text{Mn}(\text{H}_2\text{O})_4[\text{Re}_6\text{S}_8(\text{CN})_6]$ (**2**) transformation may be proposed. In **2** all the atoms rather than only the heavy ones follow the tetragonal- I motif. In the $(n\text{-Pr}_4\text{N})_2M(\text{H}_2\text{O})_5[\text{Re}_6\text{S}_8(\text{CN})_6] \cdot \text{H}_2\text{O}$

compounds ($M = \text{Mn}$, Co , Ni) the fragments $\{M(\text{H}_2\text{O})_5[\text{Re}_6\text{S}_8(\text{CN})_6]\}^{2-}$ are linked along the c axis by hydrogen bonds between O3 and N2' atoms of adjacent fragments (20). In **2** the $\{\text{Mn}(\text{H}_2\text{O})_4[\text{Re}_6\text{S}_8(\text{CN})_6]\}^{2-}$ fragments are linked by covalent N–M bonds forming the infinite chains. Therefore, the hydrogen bonds between the fragments $\{\text{Mn}(\text{H}_2\text{O})_5[\text{Re}_6\text{S}_8(\text{CN})_6]\}^{2-}$ in the molecular structure of **1** are structural precursors of the covalent bonds in extended chains found in the chain type structure. The removal of the *trans*-coordinated water molecule in the $(n\text{-Pr}_4\text{N})_2\text{Mn}(\text{H}_2\text{O})_5[\text{Re}_6\text{S}_8(\text{CN})_6] \cdot \text{H}_2\text{O}$ compound makes it possible to form a direct M–NC link to the neighboring cluster anion (see Fig. 7). This leads to removal of the solvate water molecule (O1w) and to a slight shift and tilt to organic cations. This transformation increases the

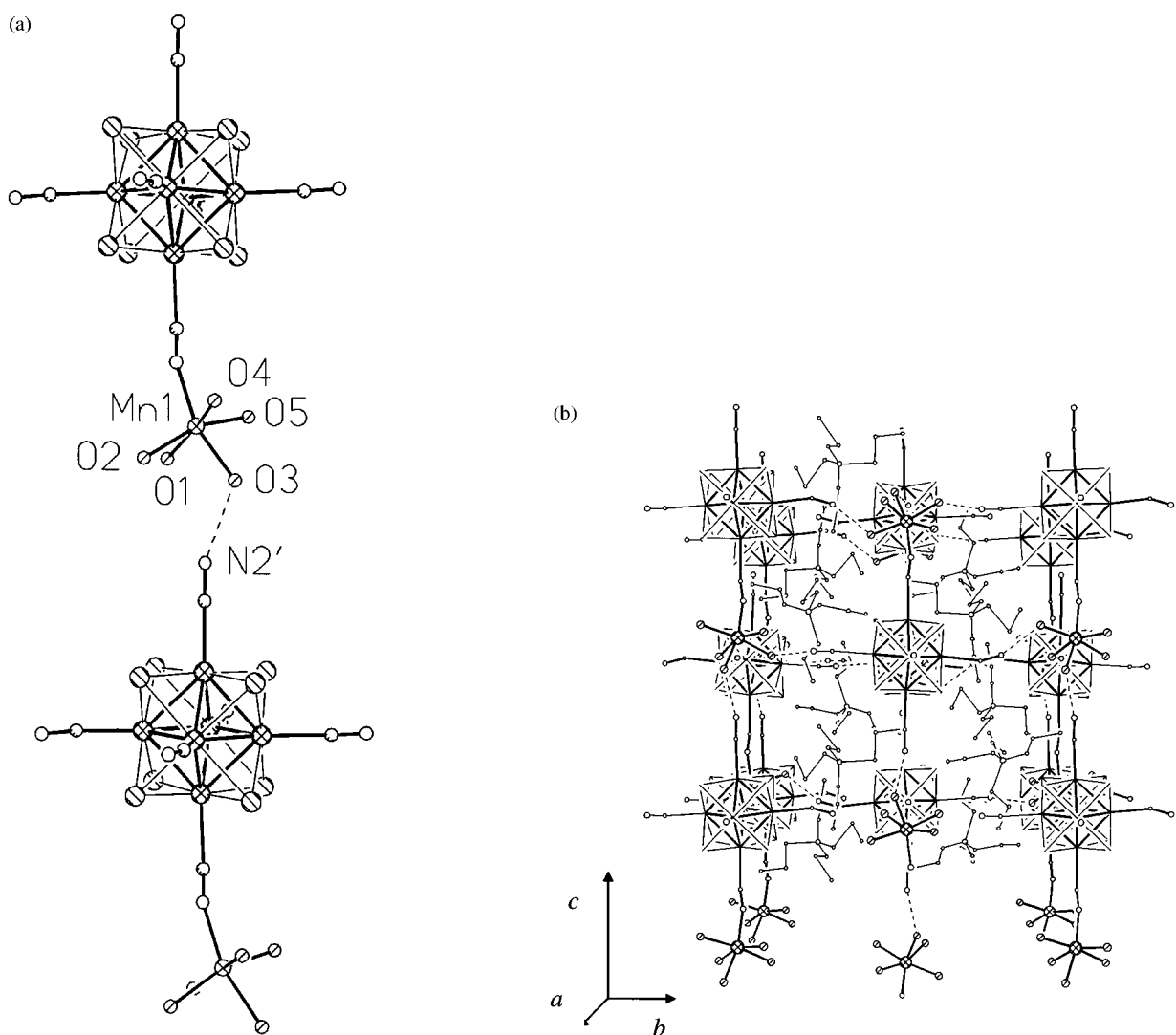


FIG. 5. Structure of $(\text{Pr}_4\text{N})_2\text{Mn}(\text{H}_2\text{O})_5[\text{Re}_6\text{Se}_8(\text{CN})_6] \cdot \text{H}_2\text{O}$. (a) Ionic pairs of $\{\text{Mn}(\text{H}_2\text{O})_5[\text{Re}_6\text{Se}_8(\text{CN})_6]\}^{2-}$ linked along the c direction by hydrogen bonds. (b) Packing of ionic pairs of $\{\text{Mn}(\text{H}_2\text{O})_5[\text{Re}_6\text{Se}_8(\text{CN})_6]\}^{2-}$ and Pr_4N^+ cations in yz projection. Hydrogen bonds are shown as dashed lines.

symmetry of the structure from $P2_12_12_1$ to $I4/m$. This model may be extended to other metals.

3.3. IR Spectra

Vibration spectra in the range $2000\text{--}2400\text{ cm}^{-1}$ reveal the presence of inequivalent CN ligands in the compounds. In the spectra of chain compounds there are two sharp bands with intensity ratio 2:1. The band with frequency $2114\text{--}2117\text{ cm}^{-1}$ corresponds to the terminal CN ligands in the structure and is consistent with the vibration frequency in the noncoordinated $[\text{Re}_6\text{S}_8(\text{CN})_6]^{4-}$ anion (2119 cm^{-1} in $\text{Cs}_3\text{K}[\text{Re}_6\text{S}_8(\text{CN})_6] \cdot 2\text{H}_2\text{O}$ (12)) (top curve in Fig. 8). The second band, shifted to the higher frequencies, corresponds

to the R-CN-M bridge. The value of the shift increases in the series Mn (2145 cm^{-1}), Co (2161 cm^{-1}), and Ni (2166 cm^{-1}) and is consistent with the Irving–Williams series. Compounds with the isolated fragments have six nonequivalent cyano ligands and their spectra are more complicated. For example, in the spectrum of $(\text{Pr}_4\text{N})_2\text{M}(\text{H}_2\text{O})_5[\text{Re}_6\text{S}_8(\text{CN})_6] \cdot \text{H}_2\text{O}$ there are at least four $\nu(\text{CN})$ vibrations: one of them corresponds to the bridging $\text{Re-C}\equiv\text{N-Ni}$ cyanide (2168 cm^{-1}), and the other three correspond to the terminal ones. Splitting of the terminal CN stretch bands is caused by hydrogen bond formation and the different environments of the cyano ligands.

The spectra of the selenocyanide compounds are similar to those of the sulfur ones but are red-shifted due to lower

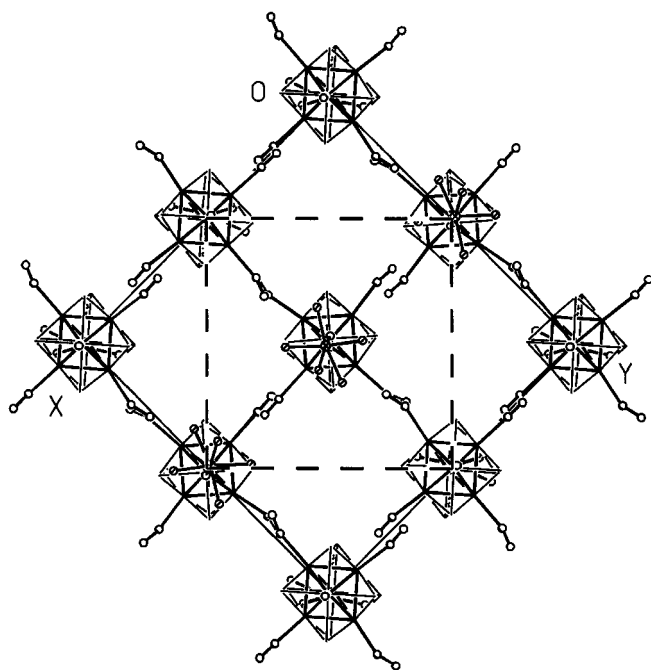


FIG. 6. The xy projection of **2** (top) and **3** (bottom) structures, Pr_4N^+ cations are omitted for clarity. The pseudotetragonal I cell in **3** is shown by dashed lines.

$\nu(\text{CN})$ stretch vibration frequencies of the noncoordinated $[\text{Re}_6\text{Se}_8(\text{CN})_6]^{4-}$ anion.

3.4. Magnetic Properties

It is well known that CN ligands are effective channels for exchange interactions (22). Nevertheless, the magnetic behavior of the obtained compounds can be described in terms of a magnetically dilute system. The effective magnetic moments μ_{eff} at room temperature correspond to spin-only values for isolated M^{2+} ($M = \text{Mn}, \text{Ni}$) ions in the high spin states with no significant interactions over the whole

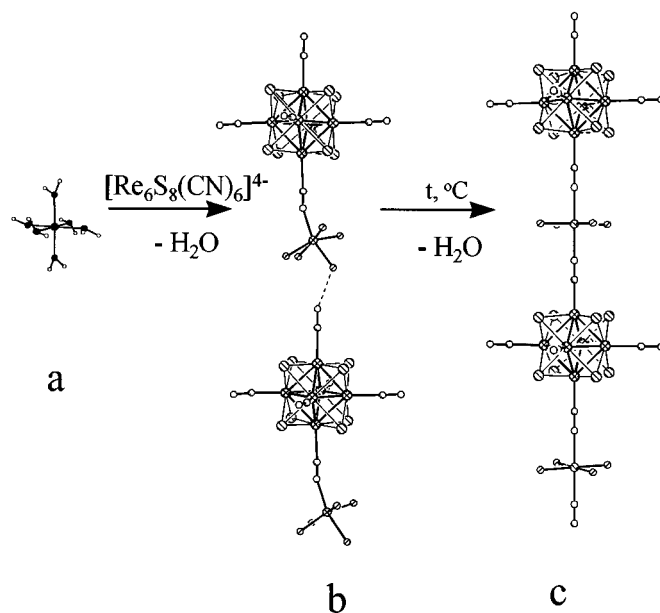


FIG. 7. Stepwise substitution of water molecules in transition metal centers: $[\text{M}(\text{H}_2\text{O})_6]^{2+}$ cation (a), $\{\text{M}(\text{H}_2\text{O})_5[\text{Re}_6\text{S}_8(\text{CN})_6]\}^{2-}$ fragments (b), and $\{\text{M}(\text{H}_2\text{O})_4[\text{Re}_6\text{S}_8(\text{CN})_6]\}_{\infty}^{2-}$ chain (c).

temperature range studied (4–300 K). The cluster cores $[\text{Re}_6\text{S}_8]^{2+}$ and $[\text{Re}_6\text{Se}_8]^{2+}$ have 24 valence cluster electrons and are diamagnetic, so they do not contribute to paramagnetic susceptibility. The absence of interactions between the M^{2+} cations indicates that the clusters also do not provide significant exchange pathways.

4. CONCLUSION

The interaction of aqueous solutions of $[\text{Re}_6\text{X}_8(\text{CN})_6]^{4-}$ ($X = \text{S}, \text{Se}$) cluster anions and transition metal aqua cations $\text{M}(\text{H}_2\text{O})_6^{2+}$ gives rise to the formation of relatively strong covalent $M\text{-NC}$ bonds instead of $M\text{-OH}_2$ bonds. Such substitution is thermodynamically favorable and should result in formation of a compound with a maximal number of $M\text{-NC}$ bonds. In the case of $[\text{Re}_6\text{X}_8(\text{CN})_6]^{4-}$ ($X = \text{S}, \text{Se}$) cluster anions this framework would have $\{\text{M}[\text{Re}_6\text{X}_8(\text{CN})_6]\}_{\infty\infty\infty}^{2-}$ stoichiometry. For steric reasons this framework does not allow the insertion of cations which are necessary to compensate the charge. Therefore, only frameworks with less than six $M\text{-NC}$ bonds are possible. In the case of Cs^+ , (11), Me_4N^+ , and Et_4N^+ salts (13) the transition metal ions form four $M\text{-NC}$ bonds. In the Pr_4N^+ salts $(\text{Pr}_4\text{N})_2\text{M}(\text{H}_2\text{O})_5[\text{Re}_6\text{X}_8(\text{CN})_6] \cdot \text{H}_2\text{O}$ and $(\text{Pr}_4\text{N})_2\text{M}(\text{H}_2\text{O})_4[\text{Re}_6\text{S}_8(\text{CN})_6]$ the metal ions make one or two $M\text{-NC}$ bonds forming structures of low dimensionality. Under mild conditions the isolated fragments $\{\text{M}(\text{H}_2\text{O})_5[\text{Re}_6\text{X}_8(\text{CN})_6]\}^{2-}$ can be transformed into infinite chains $\{\text{M}(\text{H}_2\text{O})_4[\text{Re}_6\text{X}_8(\text{CN})_6]\}_{\infty}^{2-}$.

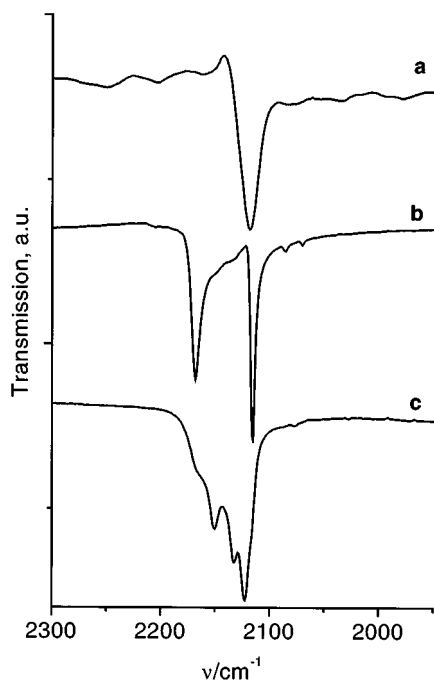
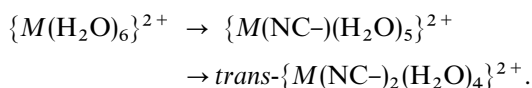


FIG. 8. IR spectra of $\text{Cs}_3\text{K}[\text{Re}_6\text{S}_8(\text{CN})_6] \cdot 2\text{H}_2\text{O}$ (a), $(\text{Pr}_4\text{N})_2\text{Ni}(\text{H}_2\text{O})_4[\text{Re}_6\text{S}_8(\text{CN})_6]$ (b) and $(\text{Pr}_4\text{N})_2\text{Ni}(\text{H}_2\text{O})_5[\text{Re}_6\text{S}_8(\text{CN})_6] \cdot \text{H}_2\text{O}$ (c).

This process can be explained in terms of stepwise substitution of water molecules in the aqua cations (Fig. 7):



In the first step one water molecule is substituted by the cyano ligand and kinetically stable insoluble $(\text{Pr}_4\text{N})_2M(\text{H}_2\text{O})_5[\text{Re}_6\text{S}_8(\text{CN})_6] \cdot \text{H}_2\text{O}$ is precipitated. Heating the precipitate in water results in substitution of the second water molecule located in the position *trans* to CN ligand and in formation of infinite chains in $(\text{Pr}_4\text{N})_2M(\text{H}_2\text{O})_4[\text{Re}_6\text{S}_8(\text{CN})_6]$.

ACKNOWLEDGMENTS

This work was supported by the Russian Foundation for Basic Research (Grant No. 99-03-32789) and special donation for young scientists from Siberian Branch of Russian Academy of Sciences. The authors

thank Dr. V. N. Ikorskii (Institute of Inorganic Chemistry) for magnetic measurements.

REFERENCES

1. K. R. Dunbar and R. A. Heintz in "Progress in Inorganic Chemistry" (K. D. Karlin, Ed.), Vol. 45, p. 283, Wiley, New York, 1997.
2. T. Iwamoto, in "Comprehensive Supramolecular Chemistry" (J. L. Atwood, J. E. D. Davies, D. D. Macnicol, and F. Vögtle, Eds.), Vol. 6, p. 643, Pergamon, Elmsford, NY, 1996.
3. B. H. Chadwick and A. G. Sharpe, in "Advances in Inorganic and Radiochemistry" (H. J. Emeléus and A. G. Sharpe, Eds.), Vol. 8, p. 83, Academic Press, New York, 1996.
4. H. Yuge and T. Iwamoto, *J. Chem. Soc., Dalton Trans.* 1237 (1994).
5. M. Ohba, H. Okawa, T. Ito, and A. Ohto, *J. Chem. Soc., Chem. Commun.* 1545 (1995).
6. H. Miyasaka, H. Ieda, N. Matsumoto, N. Re, R. Crescenzi, and C. Florani, *Inorg. Chem.* **37**, 255 (1998).
7. Yu. V. Mironov, A. V. Virovets, V. E. Fedorov, N. V. Podberezskaya, O. V. Shishkin, and Yu. T. Struchkov, *Polyhedron* **14**, 3171 (1995).
8. N. G. Naumov, A. V. Virovets, N. V. Podberezskaya, and V. E. Fedorov, *Russ. J. Struct. Chem.* **38**, 857 (1997).
9. H. Imoto, N. G. Naumov, A. V. Virovets, T. Saito, and V. E. Fedorov, *Russ. J. Struct. Chem.* **39**, 720 (1997).
10. Yu. V. Mironov, J. A. Cody, T. E. Albrecht-Schmitt, and J. A. Ibers, *J. Am. Chem. Soc.* **119**, 493 (1997).
11. N. G. Naumov, A. V. Virovets, M. N. Sokolov, S. B. Artemkina, and V. E. Fedorov, *Angew. Chem., Int. Ed.* **37**, 1943 (1998).
12. N. G. Naumov, A. V. Virovets, Yu. I. Mironov, S. B. Artemkina, and V. E. Fedorov, *Ukr. Khim. Zh.* **65**, 21 (1999).
13. N. G. Naumov, A. V. Virovets, S. B. Artemkina, D. Yu. Naumov, Ju. A. K. Howard, and V. E. Fedorov, *Supramol. Chem.*, in press.
14. L. G. Beauvais, M. P. Shores, and J. R. Long, *Chem. Mater.* **10**, 3783 (1998).
15. M. P. Shores, L. G. Beauvais, and J. R. Long, *Inorg. Chem.* **38**, 1648 (1999).
16. C. Fischer, S. Feichter, H. Tributsch, G. Reck, and B. Schultz, *Ber. Bunsenges. Phys. Chem.* **96**, 1652 (1992).
17. A. Perrin, L. Leduc, and M. Sergent, *Eur. J. Solid State Chem.* **28**, 119 (1991).
18. A. Altomare, M. C. Burla, M. Camalli, G. L. Cascarano, C. Giacovazzo, A. Guagliardi, A. G. G. Moliterni, G. Polidori, and R. Spagna, *J. Appl. Crystallogr.* **32**, 115 (1999).
19. G. M. Sheldrick, SHELX-97, Release 97-2, University of Goettingen, Germany, 1998.
20. N. G. Naumov, S. B. Artemkina, A. V. Virovets, and V. E. Fedorov, *Solid State Sci.* **1**, 463 (1999).
21. J. R. Long, L. S. McCarty, and R. H. Holm, *J. Am. Chem. Soc.* **118**, 4603 (1996).
22. O. Kahn, in "Advances in Inorganic Chemistry" (A. G. Sykes, Ed.), Vol. 43, p. 179, Academic Press, New York, 1995.